Automated subpixel snow parameter mapping with AVIRIS data

Thomas H. Painter[1,2], Dar A. Roberts[1,2], Jeff Dozier[2,3], Robert O. Green[1,2,4]

[1]Department of Geography, University of California, Santa Barbara 93106

[2]Institute for Computational Earth System Science, University of California, Santa Barbara 93106

[3]Donald Bren School of Environmental Science and Management, University of California, Santa Barbara 93106

[4]Jet Propulsion Laboratory, California Institute of Technology, Pasadena, CA 91109

ABSTRACT

We describe an automated algorithm (MEMSCAG) for mapping subpixel snow covered area (SCA) and snow grain size with AVIRIS data. The algorithm is based on the multiple endmember approach to spectral mixture analysis in which the spectral endmembers and the number of endmembers can vary on a pixel-by-pixel basis. This approach accounts for surface cover heterogeneity within a scene. The mixture analysis runs on endmembers from a spectral library of snow, vegetation, rock, soil, and lake ice spectra. Snow endmembers of varying grain size were produced with a radiative transfer model. All non-snow endmembers were collected with a portable field spectrometer. Mapping is performed through sequential 2-endmember, 3-endmember, and 4-endmember mixture model runs, each subject to constraints on RMS, residuals, fractions and priority. Grain size is determined by the grain size of the snow endmember used in the optimal mixture model. We apply MEMSCAG to AVIRIS data collected over Mammoth Mountain, CA and the northern site of the BOREAS in Manitoba, Canada. MEMSCAG produces appropriate snow covered area estimates in all regions. A preliminary comparison of grain size estimates from MEMSCAG with field measurements demonstrates high accuracy.

INTRODUCTION

Maps of snow covered area and grain size provide initialization, validation, and re-initialization for distributed climatologic and snowmelt models. Snow cover is likely to be a sensitive indicator of climate change. Snow grain size is a dominant control over the spectral albedo, hence its spatial distribution can strongly influence the surface net radiation at a range of scales.

The spectral signature of pure snow is primarily sensitive to grain size (Figure 1). With an increase in particle size, visible reflectance remains unchanged while near infrared and short wave infrared reflectance decrease. This is due to a six order of magnitude change in the imaginary part of the complex index of refraction of ice across the solar spectrum. Mountainous regions frequently exhibit grain size gradients driven by gradients in air temperature and incident solar radiation. Due to the sensitivity of the spectral signature to particle size, snow exhibits a gradient in spectral signature along the grain size gradients.

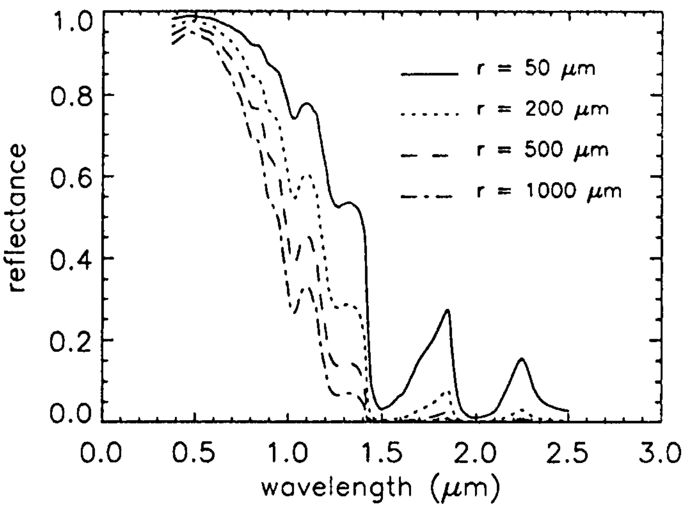

Figure 1. Directional-hemispherical reflectance of snow for varying grain size.

The efficacy of spectral mixture analysis in mapping subpixel surface cover has been shown for snow (Nolin *et al.*, 1993; Rosenthal and Dozier, 1996), vegetation (Roberts *et al.*, 1993), and geology (Adams *et al.*, 1986). In previous work (Painter *et al.*, 1996; Painter *et al.*, 1998), we demonstrated that a suite of snow endmembers varying with grain size is required to accurately map snow covered area and grain size with spectral mixture analysis. Roberts *et al.* (1998) presented multiple endmember spectral mixture analysis (MESMA), in which endmembers and the number of endmembers are allowed to vary pixel by pixel. This approach can better account for surface cover heterogeneity than ordinary spectral mixture analysis in which a suite of endmembers is selected to model the entire scene.

ALGORITHM

The automated algorithm MEMSCAG (Multiple EndMember Snow Covered Area and Grain size) is based on the MESMA approach. We created a spectral library of snow, vegetation, rock, soil, lake ice, and vegetation-shaded snow spectra. Snow spectra were generated using a two stream radiative transfer model (Wiscombe and Warren, 1980). The Mie scattering parameters were generated for ice spheres of radii ranging from 50 to 1500 μm (Wiscombe, 1980). Vegetation, rock, soil, lake ice, and vegetation-shaded snow spectra were acquired in the central Sierra Nevada with an Analytical Spectral Devices FieldSpec FR field spectroradiometer. Field spectra were subsequently convolved to AVIRIS bandpasses. AVIRIS calibrated radiance was converted to apparent surface reflectance using the nonlinear least squares water vapor fitting of Green *et al.* (1993).

The algorithm flow is shown in Figure 2. We run suites of n endmember models in which the first n-1 endmembers are physical constituents (snow, vegetation, rock, etc.) and the nth endmember is photometric shade. For example, a two endmember model could consist of snow (r = 750 μm) and shade, and determines if the pixel is pure snow with grain size of 750 μm. In order for a model to be accepted for a pixel, the model must meet the following constraints: RMSE < 2.5%, no 7 consecutive residuals can exceed 2.5%, and spectral fractions must be between –0.01 and 1.01. For each n, some pixels have multiple models that meet the constraints (overlapping models). To select the optimal model, we use the minimum RMSE as a metric. This produces best fit SCA and grain size images for each n. In order to select from overlapping models across varying n, we use priority selections. Priorities were initially established, from highest to lowest, as two, three, and four endmembers. For example, if a pixel is modeled in the two, three, and four endmember case, its SCA and grain size derive from the values of the two endmember case.

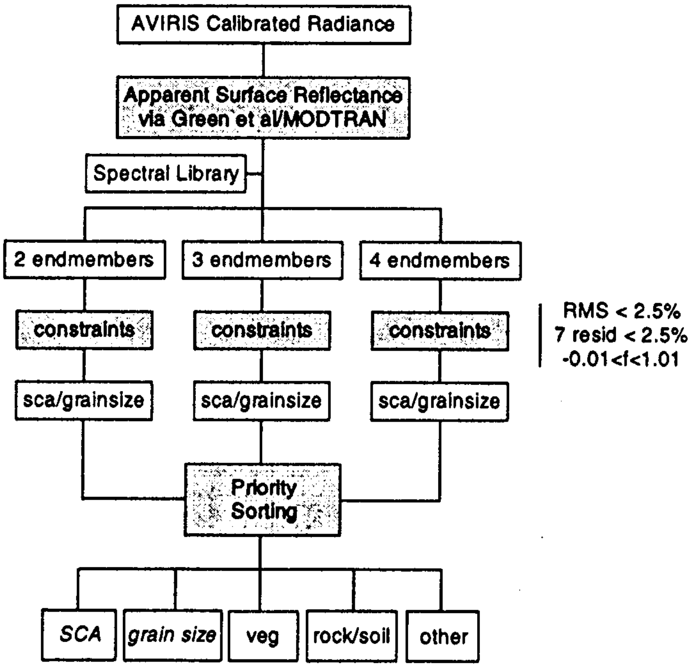

MEMSCAG = Multiple Endmember Snow Covered Area and Grain Size

Figure 2 Flowchart of MEMSCAG algorithm.

The establishment of priorities deserves further attention in order to preserve geographic and physical consistency. A likely geographic and spectral scenario is snow mixed spatially with rock, whereas an unlikely scenario is that of snow mixed with illuminated vegetation. Vegetation vertical relief dictates that the latter mixture includes vegetation-shaded snow, a third physical constituent. Hence, the four endmember model (snow, vegetation, vegetation-shaded snow, and shade) is more realistic than the three endmember model.

RESULTS

We applied MEMSCAG to AVIRIS data acquired over Mammoth Mountain, CA and the northern BOREAS site, Manitoba, Canada on April 5, 1994 and April 20, 1994. Figures 3 and 4 show SCA and grain size results for Mammoth Mountain and BOREAS,

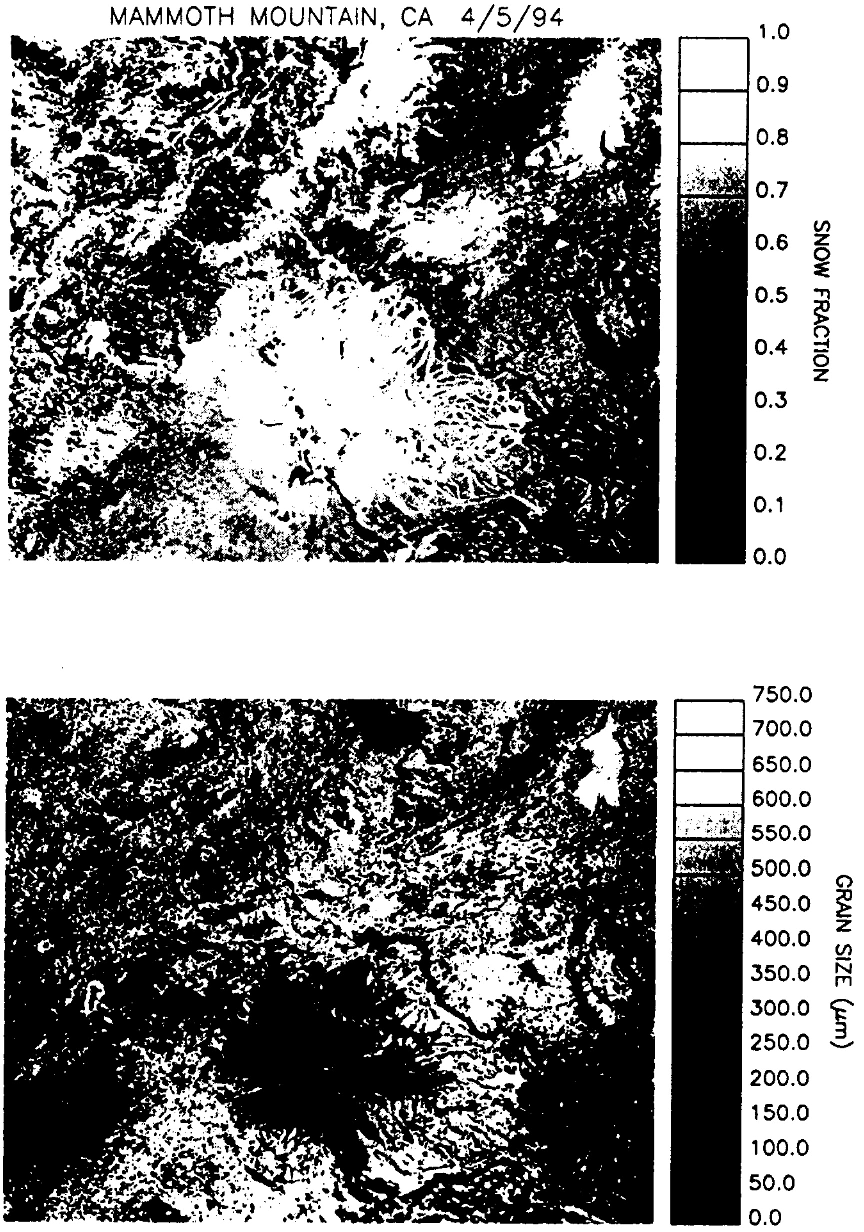

Figure 3 Subpixel snow covered area and grain size for Mammoth Mountain, CA - 4/5/94.

respectively. SCA results were appropriate for both regions, exhibiting high snow cover above timberline and in large forest openings. Lower snow cover fractions corresponded

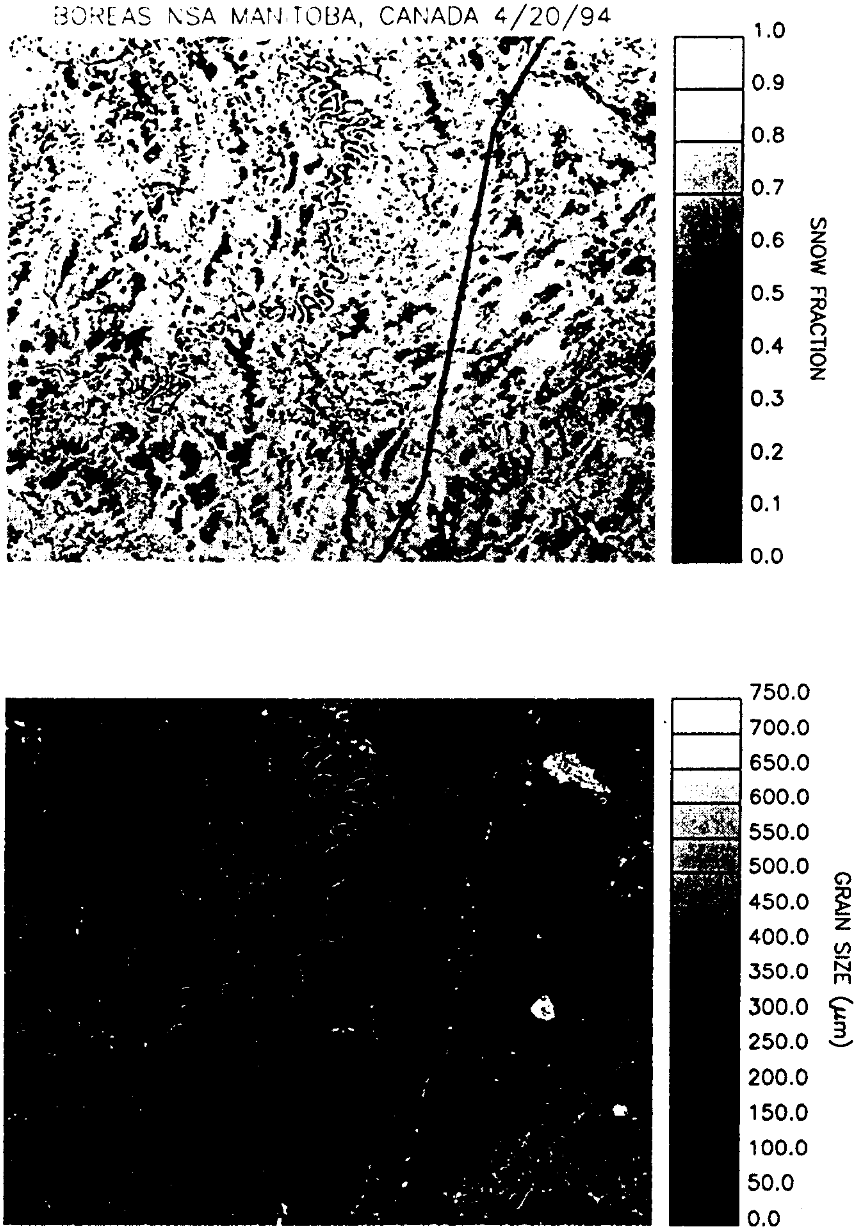

Figure 4 Subpixel snow covered area and grain size for BOREAS northern site - 4/20/94.

to timbered regions, and exposed rock outcrops, roads and lake ice. Surface grain sizes in the boreal forest vary according to canopy closure, with larger grains in openings exposed to greater temporally-integrated solar irradiance. Grain sizes in the boreal forest as retrieved by MEMSCAG were qualitatively consistent with field measurements. Table 1 presents a preliminary comparison of grain sizes retrieved by MEMSCAG with those retrieved from stereological (Davis *et al.*, 1987) analysis of snow samples collected on Mammoth Mountain. Though not statistically significant, the results demonstrate potentially high accuracy. Root mean squared error for this sample is 23.6 μm.

Mammoth Mtn. 4/5/94	**MEMSCAG grain radius (μm)**	**STEREOLOGY grain radius (μm)**
Back Chair 23	124.1	130.5
Boundary	240.7	281.1
Climax	80.4	81.4

Table 1 Comparison of MEMSCAG and stereology grain size results for Mammoth Mountain, CA - 4/5/94.

ACKNOWLEDGMENTS

This work was sponsored under NASA EOS MTPE grant NAGW-5185 and performed at the University of California, Santa Barbara and the Jet Propulsion Laboratory, Pasadena, CA. We thank Robert E. Davis of the U.S. Army Corps of Engineers Cold Regions Research and Engineering Laboratory for processing snow samples.

REFERENCES

Adams, J. B., M. O. Smith, and P. E. Johnson, 1986, Spectral mixture modeling: A new analysis of rock and soil types at the Viking Lander 1 site, *J. Geophys. Res.* 91(B8):8098-8112.

Davis, R. E., J. Dozier, and R. Perla, 1987, Measurement of snow grain properties, in *Seasonal Snowcovers: Physics, Chemistry, Hydrology,* H. G. Jones and W.J. Orville-Thomas, eds., pp 63-74, NATO ASI Series, D. Reidel Publishing Company.

Green, R. O., J. E. Conel, and D. A. Roberts, 1993, Estimation of aerosol optical depth and calculation of apparent surface reflectance from radiance measured by the Airborne Visible/Infrared Imaging Spectrometer (AVIRIS) using MODTRAN2, *SPIE Conf. No. 1937, Imaging Spectrometry of the Terrestrial Environment,* p.12.

Nolin, A. W., J. Dozier, and L. A. K. Mertes, 1993, Mapping alpine snow using a spectral mixture modeling technique, *Ann. Glaciol.* 17:121-124.

Painter, T. H., D. A. Roberts, R. O. Green, and J. Dozier, 1996, Subpixel snow covered area and snow grain size from mixture analysis with AVIRIS data, *Summaries of the Sixth Annual JPL Airborne Earth Science Workshop, R. O. Green, editor, JPL Publication 96-4, Vol. 1*, 185-188.

Painter, T. H., D. A. Roberts, R. O. Green, and J. Dozier, 1998, Improving spectral mixture analysis of snow covered area with AVIRIS data, *Remote Sens. Environ.*, in press.

Roberts, D. A., M. O. Smith, and J. B. Adams, 1993, Green Vegetation, Non-photosynthetic Vegetation, and Soils in AVIRIS Data, *Remote Sens. Environ.* 44(2/3):255-269.

Roberts, D. A., M. Gardner, R. Church, S. Ustin, G. Scheer and R. O. Green, 1998, Mapping chaparral in the Santa Monica Mountains using multiple endmember spectral mixture models, *Remote Sens. Environ.*, in press.

Rosenthal, W., and J. Dozier, 1996, Automated mapping of montane snow cover at subpixel resolution from the Landsat Thematic Mapper, *Water Resour. Res.* 32(1):115-130.

Wiscombe, W., and S. G. Warren, 1980, A model for the spectral albedo of snow I. Pure snow, *J. Atmos. Sci.* 37:2712-2733.

Wiscombe, W., 1980, Improved Mie scattering algorithms, *Applied Optics* 19:1505-1509.